

Semi-Automated Analysis of Foveal Maturity in Premature and Full-Term Infants Using Handheld Swept-Source Optical Coherence Tomography

Sumner E. Lawson¹, Emily K. Tam^{2,3}, Yujiao Zheng⁴, Teng Liu⁴, Tatiana R. Monger², Karen E. Lee⁵, Alex Legocki³, John Kelly², Leona Ding³, Ruikang K. Wang^{3,4}, Kristina Tarczy-Hornoch^{2,3}, and Michelle T. Cabrera^{2,3}

¹ University of Washington School of Medicine, Seattle, WA, USA

² Division of Ophthalmology Seattle Children's Hospital, Seattle, WA, USA

³ Department of Ophthalmology, University of Washington, Seattle, WA, USA

⁴ Department of Bioengineering, University of Washington, Seattle, WA, USA

⁵ Pediatric Ophthalmology Service, Wills Eye Hospital, Philadelphia, PA, USA

Correspondence: Michelle T. Cabrera, OA.9.220 Ophthalmology, 4800 Sand Point Way NE, Seattle, WA 98105, USA.

e-mail: cabreram@uw.edu

Received: October 17, 2022

Accepted: January 25, 2023

Published: March 7, 2023

Keywords: foveal development; optical coherence tomography (OCT); retinopathy of prematurity

Citation: Lawson SE, Tam EK, Zheng Y, Liu T, Monger TR, Lee KE, Legocki A, Kelly J, Ding L, Wang RK, Tarczy-Hornoch K, Cabrera MT. Semi-automated analysis of foveal maturity in premature and full-term infants using handheld swept-source optical coherence tomography. *Transl Vis Sci Technol.* 2023;12(3):5. <https://doi.org/10.1167/tvst.12.3.5>

Purpose: To develop a semi-automated method of measuring foveal maturity using investigational handheld swept source-optical coherence tomography (SS-OCT).

Methods: In this prospective, observational study, full-term newborns and preterm infants undergoing routine retinopathy of prematurity screening were imaged. Semi-automated analysis measured foveal angle and chorioretinal thicknesses at the central fovea and average two-sided parafovea by three-grader consensus, correlating with OCT features and demographics.

Results: One hundred ninety-four imaging sessions from 70 infants were included (47.8% girls, 37.6 ± 3.4 weeks postmenstrual age, 26 preterm infants with birth weight 1057 ± 325.0 , gestational age 29.0 ± 3.0 weeks). Foveal angle (96.1 ± 22.0 degrees) steepened with increasing birth weight ($P = 0.003$), decreasing inner retinal layer thickness, and increasing gestational age, postmenstrual age, and foveal and parafoveal choroidal thickness (all $P < 0.001$). Inner retinal fovea/parafovea ratio (0.4 ± 0.2) correlated with increasing inner foveal layers, decreasing postmenstrual age, gestational age, and birth weight (all $P < 0.001$). Outer retinal F/P ratio (0.7 ± 0.2) correlated with ellipsoid zone presence ($P < 0.001$), increased gestational age ($P = 0.002$), and birth weight ($P = 0.003$). Foveal (447.8 ± 120.6 microns) and parafoveal (420.9 ± 109.2) choroidal thicknesses correlated with foveal ellipsoid zone presence ($P = 0.007$ and $P = 0.01$, respectively), postmenstrual age, birth weight, gestational age, and decreasing inner retinal layers (all $P < 0.001$).

Conclusions: Foveal development is dynamic and partially observed through semi-automated analysis of handheld SS-OCT imaging.

Translational Relevance: Semi-automated analysis of SS-OCT images can identify measures of foveal maturity.

Introduction

The fovea is the primary sensory location for high spatial resolution as well as color vision in the eye. Foveal development occurs in seven phases. Phases 1

and 2 are seen soon after preterm birth, whereby the outer nuclear layer is slightly concave and the fovea relatively thickened. Phases 3 and 4 occur around term and are notable for thinning of the ganglion cell layer, inner plexiform layer, and inner nuclear layers at the fovea, with thickening of the ganglion cell layer and inner plexiform layer peripherally. In phases 5 through

7, which occur in children, the ganglion cell layer and inner plexiform layers continue to thin at the fovea, with the inner nuclear layer thinning in the shoulders in phase 7. Once fully developed, the central fovea includes only the photoreceptor and nerve fiber layer, excluding all other layers.¹

Premature birth, especially before 28 weeks' gestation, has been associated with failure of the inner retinal layers to move centrifugally from the fovea, leading to an immature and shallow foveola.²⁻⁵ Previous studies have found that prematurity is the most influential factor in predicting abnormal foveal development.^{3,6}

Only one prior study reported semi-automated analysis of foveal maturity using handheld swept-source optical coherence tomography (SS-OCT) imaging.⁷ However, that study did not exclude macular edema, which may significantly impact foveal measurements. More detailed analyses of inner and outer retinal and choroidal thickness measurements have not been performed in the newborn and may improve our understanding of in vivo foveal development.

In this study, we utilize an investigational handheld, non-contact, SS-OCT device developed in house⁸⁻¹¹ to image full-term newborns and preterm infants being screened for retinopathy of prematurity (ROP). Here, we introduce a novel semi-automated method for measuring retinal and choroidal parameters correlated with foveal maturity on SS-OCT images.

Methods

This is a prospective, observational study including full-term newborns and premature infants undergoing routine ROP screening. Institutional review board approval was obtained at the University of Washington and Seattle Children's Hospital. Participants were recruited between March 2018 and June 2019 and informed consent was obtained from guardians of all participating infants after explanation of the nature and possible consequences of the study. Preterm infants were selected based on standard screening criteria for infants at risk for ROP (less than 30 weeks' gestation and/or under 1500 g birth weight). Full-term infants included in the study had at least 37 weeks' gestation and were at least 12 hours old. Infants with uncertain guardianship, systemic disease, or who had complex social situations were excluded from the study. Demographic information for participants was gathered from the medical record.

An investigational handheld SS-OCT device^{8,9} was used to obtain images on unsedated preterm infants

on the same day that they received their routine ROP screening. The device was powered by a 1060 nm swept laser source that delivers an imaging speed of 200,000 A-scans per second (200 kHz), with a spatial resolution of 5.5 μm axially and 15 μm laterally.

Follow-up took place according to standard ROP protocol, typically every 2 weeks for 2 to 7 visits. In contrast, full-term infants were imaged only once from 12 to 72 hours after birth. One to 2 drops of 1% phenylephrine hydrochloride and 0.2% cyclopentolate ophthalmic solution were used to dilate the eyes of all the participants. The handheld device includes a pupil-finding feature, which allows the operator to efficiently align the device with the awake infants' optical axis. Imaging was performed without an eyelid speculum or ocular contact. Eyelids were held open by the imagers' fingers.

Image Analysis

Two independent, trained, masked graders (authors T.R.M. and S.E.L.) selected and analyzed the highest quality OCT volumes for each eye of each infant visit using ImageJ (National Institute of Health, USA). For all disagreements between the two graders, a third masked grader (author M.T.C.) was used as a tiebreaker for the following features: cystoid macular edema (+/- altering foveal contour), subretinal fluid, persistent inner retinal layers at the fovea (graded as 0 - none, 1 - inner nuclear layer, 2 - inner plexiform layer, 3 - ganglion cell layer, and 4 - unknown), and presence of a foveal ellipsoid zone. The single best image from each OCT volume on ImageJ was selected for semi-automated analysis by two-grader consensus using two new graders (authors E.K.T. and K.E.L.).

Semi-Automated Analysis

The semi-automated analysis of the SS-OCT images was completed independently by two trained graders (authors E.K.T. and K.E.L.) using a MATLAB (MATLAB; MathWorks, Inc.) program that was developed for analysis of foveal maturity (Fig. 1).¹² Images were excluded from this analysis if they had cystoid macular edema that altered foveal contour or subretinal fluid as determined by three-grader consensus (authors T.R.M., S.E.L., and M.T.C.). Images were also excluded for any motion artifact or decentration that precluded segmentation of the fovea and parafovea as determined by two-grader consensus (authors E.K.T. and K.E.L.).

The first step was completed by uploading the previously selected best OCT image to MATLAB. This program identified the most shallow retinal

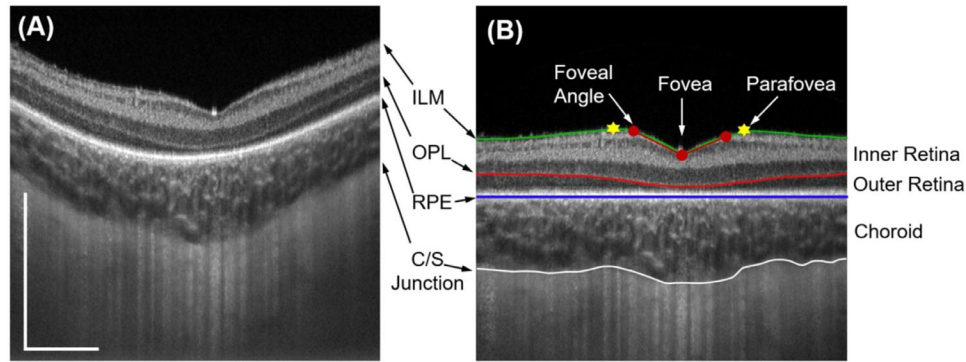


Figure 1. Illustration of measurements by semi-automated analysis of foveal maturity. **(A)** Original OCT B-scan image encompassing the foveal center. **(B)** The program automatically segmented the ILM (green curved line), OPL (red curved line), RPE (blue line), and C/S junction (white curved line). Foveal angle was measured from the brim of the foveal depression (red dots on each side) to the center of the fovea (central red dot). Inner retina was measured from the ILM to the OPL. Outer retina was measured from the OPL to the RPE. Choroid was measured from RPE to the C/S junction. The program then aligned the B-scan with the RPE as the reference (i.e., making the RPE as a straight line as shown). The thickness measurements were performed at the three locations marked by central red dot and yellow asterisks for the foveal and parafoveal thickness, respectively. ILM, internal limiting membrane; OPL, outer plexiform layer; RPE, retinal pigment epithelium; C/S, choroid/sclera border. Scale bar = 1 mm.

location in a single B scan encompassing the foveal center. Then, it automatically segmented the internal limiting membrane (ILM), outer border of the outer plexiform layer (OPL), the retinal pigment epithelium (RPE) and the choroid/sclera border (C/S junction). Finally, MATLAB automatically aligned the B-scan with the RPE as the reference (i.e., assuming the RPE to be perfectly horizontal; see Fig. 1B). Once the analysis was completed, the graders then subjectively examined the images to confirm appropriate segmentations. If there were mistakes, the script allowed the graders to make corrections as needed.

As in the study completed by de Sisternes et al. in 2015, the OCT images were segmented in a pixel-by-pixel basis at the layers defining the inner and outer retina,¹³ with the addition of choroidal thickness measurements. Following confirmation of accurate segmentation, the semi-automated program measured the inner retinal thickness (ILM to OPL), outer retinal thickness (OPL to RPE), and choroidal thickness (RPE to C/S junction^{14,15}) at 3 locations: the center of the fovea and the parafovea measured 2.5 mm from the center of the fovea to each side (see the red dots shown in Fig. 1B). Thickness measurements were automatically performed at these predefined locations by repeating measurements for each of 11 A-scans in a region centered at each location. The final thickness was obtained by averaging these 11 A-scan measurements. Foveal thicknesses were divided by the mean parafoveal thicknesses to create a fovea/parafovea (F/P) ratio for the inner and outer retinal thicknesses for each OCT volume.

The foveal angle was measured by manually selecting the foveal center (lowest point of the fovea) as well as the parafoveal points on either side whereby the retinal contour began to flatten. The program then calculated the foveal angle in degrees (see Fig. 1B). Agreement between the 2 graders was defined as a difference in thickness measurements within 50 microns and a difference in foveal angle within 15 degrees. If differences fell outside of these predetermined criteria, a third trained grader (author M.T.C.) was used as a tiebreaker, whereby the measurement closest to the tiebreaker's measurement was averaged with that of the tiebreaker's for the final result.

Statistical Analysis

A kappa score was calculated for agreement between the two graders (authors T.R.M. and S.E.L.) who performed the structural SS-OCT analysis. Intergrader agreement for the semi-automated portion of this study was completed by determining an intraclass correlation coefficient between the second set of graders (authors E.K.T. and K.E.L.) for all measurements of the complete data set.

Choroidal thicknesses (at both the fovea and mean parafovea), foveal angle, and F/P ratios for the inner and outer retinal layers were correlated with the presence of persistent inner retinal layers, ellipsoid zone, and infant-based characteristics including postmenstrual age, gestational age, and birth weight.

A generalized linear mixed model was used to account for multiple measurements for each infant (2 eyes and multiple visits) for all comparisons. For all

assessments, a P value < 0.05 was considered statistically significant. All statistical analysis was performed using SAS version 9.4 (SAS Institute, Inc., Cary, NC, USA).

Results

A total of 250 eye images from 44 full-term and 26 preterm infants were obtained in this study. Of these, 56 were excluded (15 did not contain the fovea, 16 had cystoid macular edema that altered fovea contour, 15 had subretinal fluid, and 10 had poor image quality), leaving 194 eye images for analysis (86 full-term and 108 preterm) from 44 full-term and 26 preterm infants. Demographic data for the study participants can be found in [Table 1](#).

For grading anatomic features on OCT B-scans, a kappa intergrader agreement of 1.0 was calculated, indicating complete agreement between the 2 graders. The semi-automated analysis for foveal maturity 2-grader agreement was 92/99 (92.9%). Seven images required the use of a tiebreaker. The intraclass correlation coefficients for semi-automated foveal measurements ranged from 0.81 to 0.99 ([Table 2](#)), considered “good to excellent” agreement.¹⁶

Semi-automated measurements demonstrated significantly greater foveal maturity for full-term compared to preterm infants as indicated by lower inner retinal F/P ratio (0.2 ± 0.1 vs. 0.5 ± 0.2 , respectively), lower foveal angle (81.9 ± 10.7 vs. 107.2 ± 22.3), as well as increased choroidal thickness at the fovea (508.4 ± 93.5 vs. 399.9 ± 118.3) and parafovea (473.9 ± 89.0 vs. 378.9 ± 105.6). All comparisons had

Table 2. Interclass Correlation Coefficients for Semi-Automated Analysis

Variable	ICC	95% CI	P Value
Foveal IRL* thickness	0.94	0.88–0.97	<0.001
Foveal ORL† thickness	0.86	0.81–0.89	<0.001
Parafoveal IRL thickness	0.86	0.82–0.90	<0.001
Parafoveal ORL thickness	0.81	0.61–0.78	<0.001
Foveal angle‡	0.96	0.95–0.97	<0.001
Foveal choroidal§ thickness	0.98	0.98–0.99	<0.001
Parafoveal choroidal thickness	0.99	0.98–0.99	<0.001

Abbreviations: IRL, inner retinal layer; ORL, outer retinal layer; ICC, interclass correlation coefficient; CI, confidence interval.

*IRL was measured from the internal limiting membrane to the outer plexiform layer.

†ORL was measured from the outer plexiform layer to the retinal pigment epithelium.

‡Foveal angle was measured from foveal center to two-sided foveal rim.

§Choroidal thickness was measured from the retinal pigment epithelium to the choroid/sclera junction.

a P value < 0.001 . These differences were seen in spite of largely overlapping postmenstrual age at time of imaging (see [Table 1](#)). The F/P ratio at the outer retina (0.8 ± 0.2 vs. 0.7 ± 0.2) was not associated with an infant’s preterm or full-term status ([Table 3](#)).

Among both preterm and full-term infants, increasing inner retinal F/P ratio, increasing foveal angle, and decreasing foveal and parafoveal choroidal thickness correlated with increasing persistent inner retinal layers ($P < 0.001$ for all comparisons; [Figs. 2A–C](#)), confirming their relationship with inner foveal immaturity. Ellipsoid zone presence coincided with decreasing

Table 1. Demographic Data of Study Population

Variable	Preterm	Full-Term
Total number of infants	26	44
Sex	Female = 12 (48.0%)	Female = 21 (47.7%)
Birth weight (g), mean (SD)	1057.6 (324.8)	3414.2 (501.9)
Gestational age (weeks), mean (SD)	29.09 (3.0)	39.18 (1.2)
Postmenstrual age at imaging (weeks), mean (SD)	36.08 (3.8)	39.34 (1.3)
Race/ethnicity	White = 16 (64.0%) Native American/Alaska native = 2 (8.0%) Black = 1 (4.0%) Asian = 0 (0.0%) Hispanic = 0 (0.0%) More than one = 1 (4.0%)	White = 28 (63.6%) Native American/Alaska native = 0 (0.0%) Black = 3 (6.8%) Asian = 6 (13.6%) More than one = 5 (11.4%)

Abbreviation: SD, standard deviation.

Table 3. Comparison of Foveal Parameters and Infant Preterm/Full-Term Status

Variable, Mean (SD)	Preterm	Full-Term	P Value*
N	107	84	
F/P inner retina [†]	0.5 (±0.2)	0.2 (±0.1)	<0.001
F/P outer retina [‡]	0.7 (±0.2)	0.8 (±0.2)	0.005
Foveal angle [§]	107.2 (±22.3)	81.9 (±10.7)	<0.001
Foveal choroidal thickness	339.9 (±118.3)	508.4 (±93.5)	<0.001
Parafoveal choroidal thickness	378.9 (±105.6)	473.9 (±89.0)	<0.001

Abbreviations: SD, standard deviation; N, number of individual eye visits; F/P, foveal/parafoveal ratio.

*A linear mixed model approach was used to account for multiple eyes and visits.

[†]Inner retina was measured from the internal limiting membrane to the outer plexiform layer.

[‡]Outer retina was measured from the outer plexiform layer to the retinal pigment epithelium.

[§]Foveal angle was measured from foveal center to two-sided foveal rim.

^{||}Choroidal thickness was measured from the retinal pigment epithelium to the choroid/sclera junction.

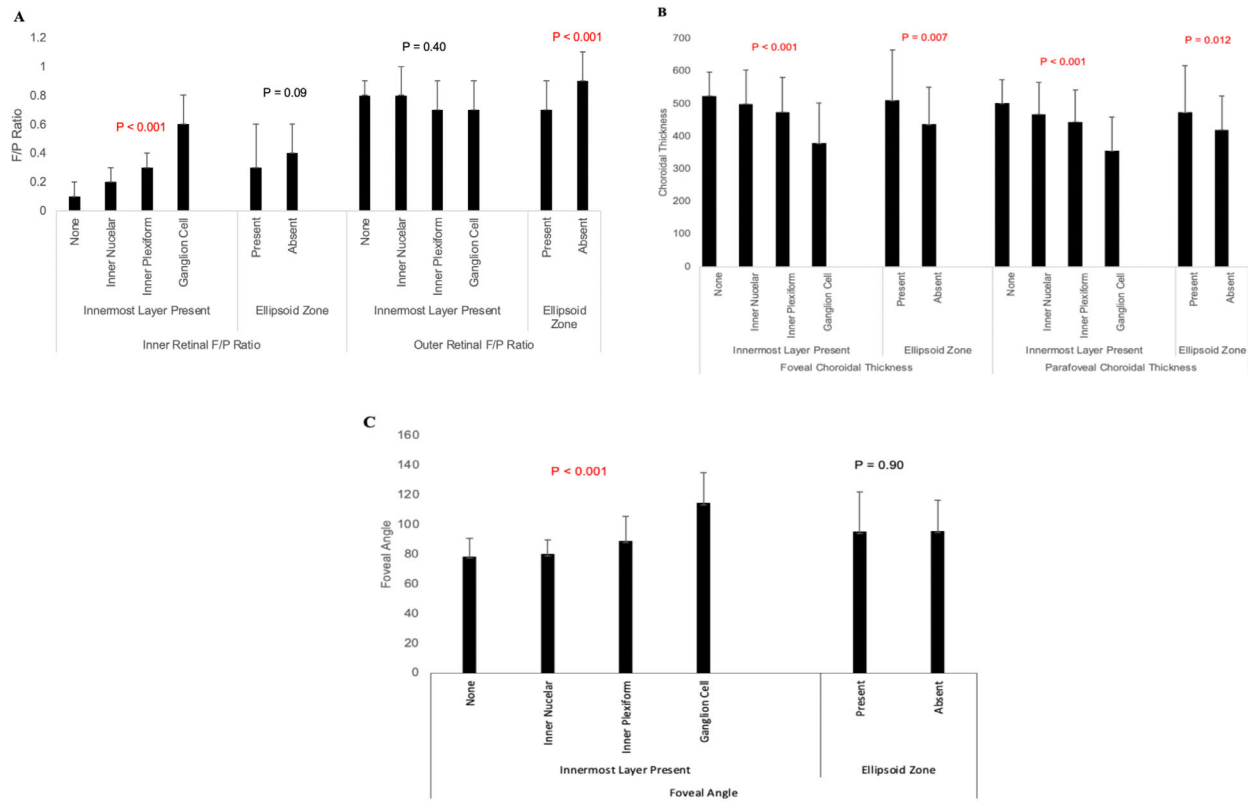


Figure 2. Semi-automated measurements of foveal maturity versus innermost layer and ellipsoid zone presence. **(A)** Mean F/P ratio at the inner retina strongly correlates with number of innermost layers present at the fovea. Mean F/P ratio at the outer retina strongly correlates with ellipsoid zone absence at the fovea. **(B)** Choroidal thickness at the fovea and parafovea correspond to absent inner retinal layers and present ellipsoid zone at the fovea. **(C)** Foveal angle increases with increasing innermost layers present at the fovea. See Figure 1 for an explanation of semi-automated measurements. Whiskers, standard deviation; F/P, fovea/parafovea ratio.

F/P ratio at the outer retina ($P < 0.001$) and increasing parafoveal ($P < 0.012$) and foveal ($P < 0.007$) choroidal thickness, suggesting that these measurements relate to outer retinal maturity (see Figs. 2A–C). Decreasing F/P ratio at the inner retina, and decreasing

foveal angle and increasing choroidal thickness at the fovea and parafovea were significantly associated with postmenstrual age at imaging, confirming strong relationships between these semi-automated measurements and maturity ($P < 0.001$; Fig. 3A). In contrast,

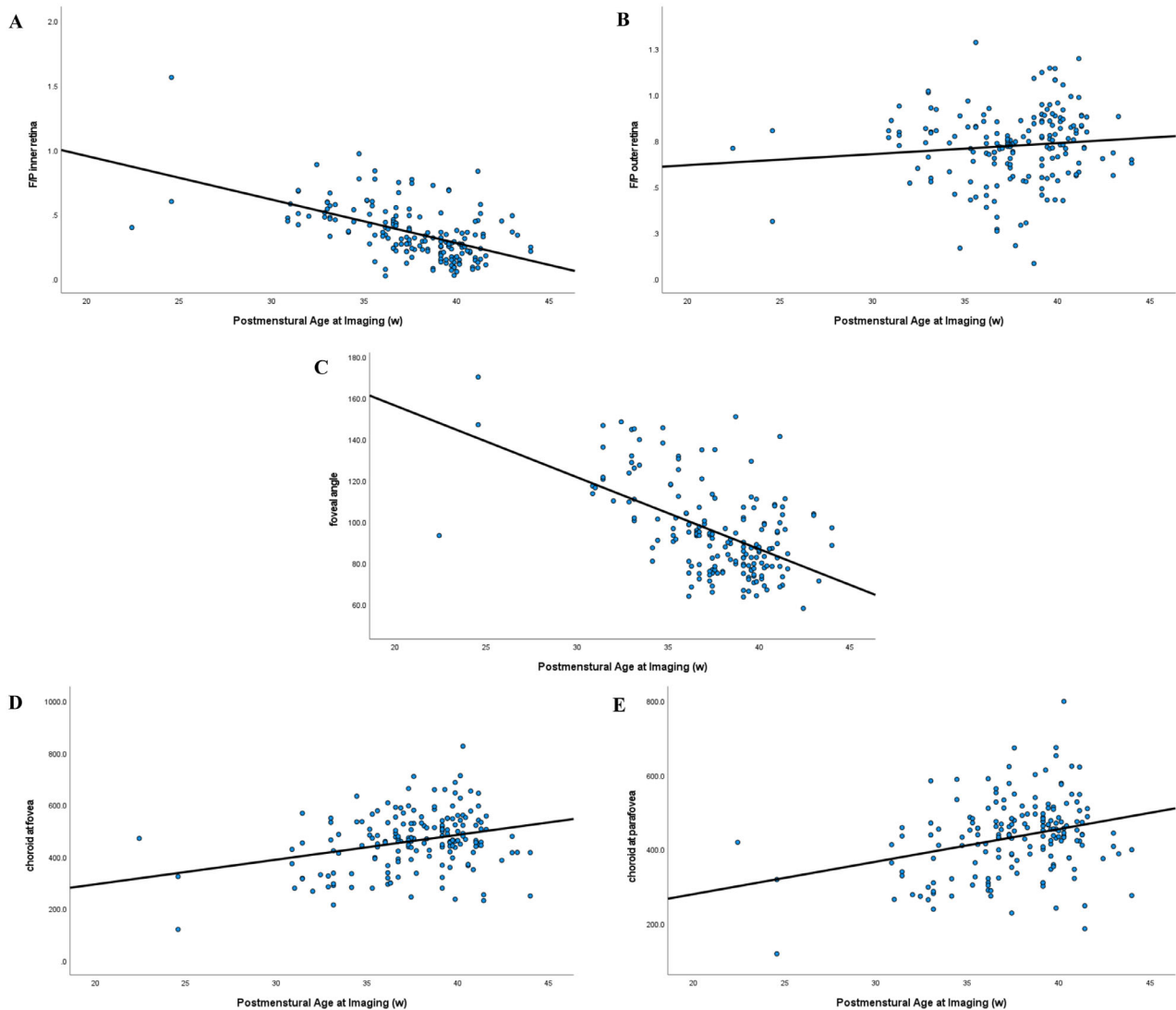


Figure 3. Semi-automated measurements of foveal maturity versus postmenstrual age. **(A)** F/P ratio at the inner retina decreases with postmenstrual age ($P < 0.001$). **(B)** F/P ratio at the outer retina increases with postmenstrual age ($P = 0.175$). **(C)** Foveal angle decreases with postmenstrual age ($P < 0.001$). **(D)** Choroidal thickness at the fovea increases with postmenstrual age ($P < 0.001$). **(E)** Choroidal thickness at the parafovea increases with postmenstrual age ($P < 0.001$). F/P, fovea/parafovea ratio; w, weeks.

the outer retinal F/P ratio did not significantly correlate with postmenstrual age at imaging (Fig. 3B). Finally, increasing gestational age and birth weight were each associated with increasing foveal maturity as measured by decreasing F/P ratio at the inner ($P = 0.001$ and $P < 0.001$, respectively) and outer retina ($P = 0.002$ and $P = 0.003$, respectively; Fig. 4A), decreasing foveal angle ($P = 0.001$ and $P < 0.001$, respectively; Fig. 4B), and increasing choroidal thickness at the fovea ($P = 0.001$ and $P < 0.001$, respectively; Fig. 4C) and parafovea ($P = 0.001$ and $P < 0.001$, respectively; see Fig. 4C). There were not adequate infants with longitudinal analysis to follow foveal development of individual infants in this study.

Discussion

This study identified correlations between known structural markers of foveal immaturity and novel semi-automated quantitative measures of foveal immaturity from handheld SS-OCT images, including F/P ratio of the inner retina, and the foveal angle and choroidal thickness at the fovea and parafovea. Although several other studies have explored foveal development with retinal segmentation and image registration,^{5,7,17} to our knowledge, this is the first study (PubMed keywords: foveal development, optical coherence tomography, and

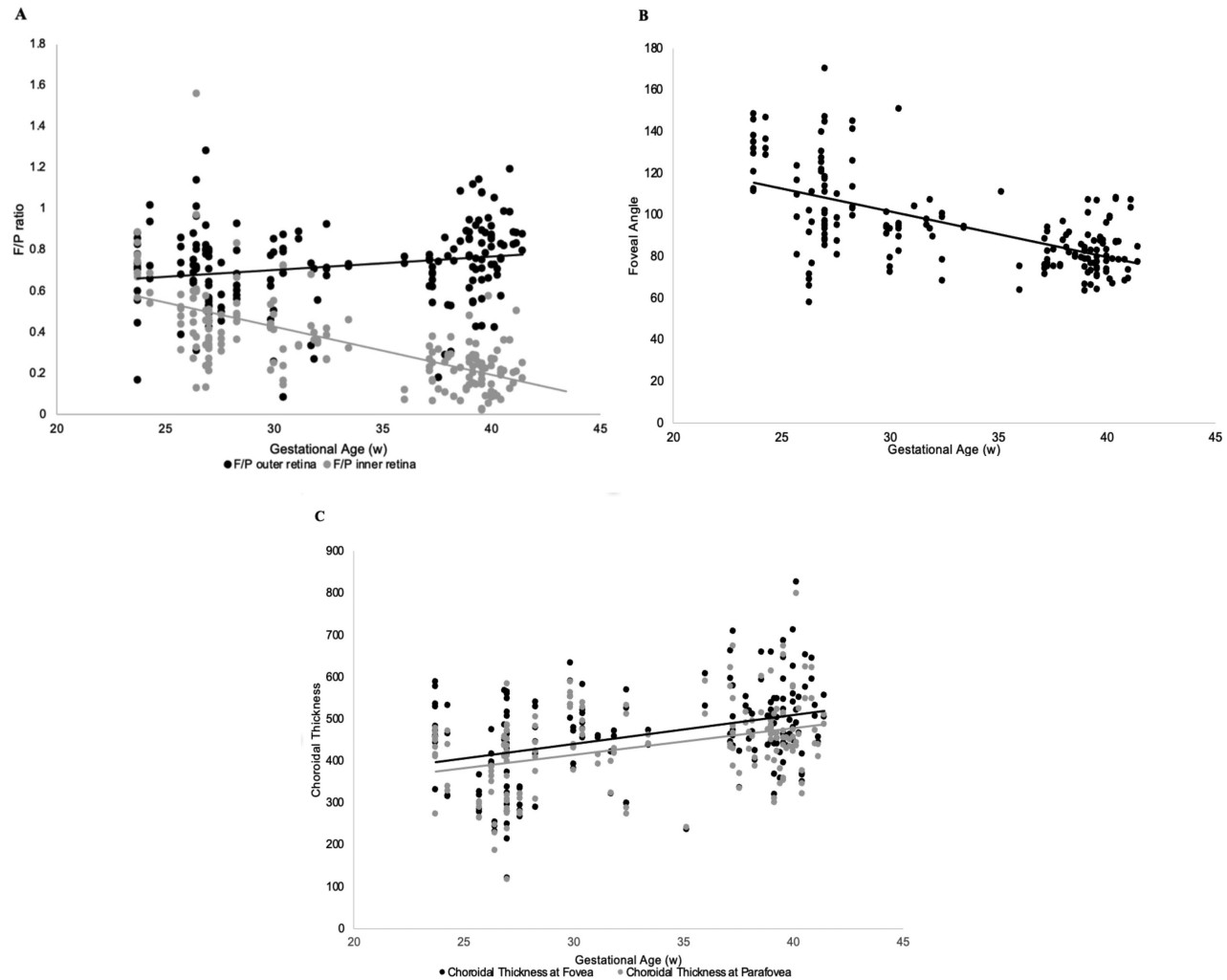


Figure 4. Semi-automated measurements of foveal maturity versus gestational age. (A) Inner retinal F/P ratio decreases whereas outer retinal F/P ratio increases with gestational age ($P < 0.001$ and $P = 0.002$, respectively). (B) Foveal angle decreases with gestational age ($P < 0.001$). (C) Choroidal thickness at both the fovea and parafovea increase with gestational age (both $P < 0.001$). F/P, fovea/parafovea ratio; w, weeks.

retinopathy of prematurity) to use this quantitative technique to segment and analyze foveal retinal and choroidal layers for awake infants in the newborn period.

Maldonado et al. analyzed premature infant foveal development using handheld spectral domain (SD)-OCT, identifying shallow foveal pit, persistent inner retinal layers, and an increased F/P ratio as signs of foveal immaturity.¹⁸ O'Sullivan et al. identified a strong correlation between neurosensory retinal total P/F ratio and postmenstrual age, gestational age, and birth weight.⁷ He et al. found that extremely preterm infants had a sustained inner retinal thickness as well as a shallow foveal pit compared to non-extremely preterm infants.⁵

Our study further explored these relationships by dividing the F/P ratio at the fovea and parafovea into inner and outer retina F/P ratios, finding that only increasing inner retinal F/P ratio correlated with persistent inner retinal layers, decreasing postmenstrual age, and decreasing birth weight.

The association between shallow fovea and immaturity is well-established.^{2,3,5,19} Yanni et al. found that the foveal pits of ex-preterm children were significantly shallower and less steep compared to those of full-term children, with greater overall retinal thickness.¹⁹ The present study found that increasing foveal angle (a quantification of this immature shallow configuration) correlates with established features of foveal immaturity, including the presence of persistent inner retinal

layers, as well as decreasing postmenstrual age, gestational age, and birth weight (all $P < 0.001$).

Choroidal thickness measurements and their relationship to foveal maturity have not been well explored previously in the newborn preterm population. The present study identified a strong relationship between foveal or parafoveal choroidal thickness and postmenstrual age, gestational age, and birth weight among both full-term and preterm infants (all $P < 0.001$), as seen previously in mostly older ex-premature children.^{14,15,20,21} The present study also found that thinner foveal and parafoveal choroidal thickness coincided with anatomic measures of foveal immaturity, including persistent inner retinal layers (both $P < 0.001$), and absent foveal ellipsoid zone ($P = 0.007$ and $P = 0.012$, respectively). Huang et al. studied choroidal thickness in term infants through SS-OCT images and found that thinner choroid was associated with an absent ellipsoid zone.¹⁰ Altogether, these findings suggest that choroidal and retinal development are linked.

The literature on the impact of foveal immaturity and decreased visual acuity is mixed.^{2,22–24} Balasubramanian et al. found that 226 eyes of young adult former preterm infants had thicker inner and outer retinal layers at the central fovea compared to 128 age-matched full-term control eyes, but only increased inner retinal layer thickness was associated with worse visual acuity.²² In contrast, Lee et al. found that outer greater than inner central foveal thicknesses correlated with visual acuity among preschool-aged ex-preterm and full-term infants.²³ Yanni et al. studied 24 preterm infants and 34 full-term controls and found that although prematurity was associated with reduced visual acuity, there was no association between visual acuity and foveal pit depth, diameter, or slope.¹⁹ Finally, Wu et al. found an association among visual acuity, foveal thickness, and volume that resolved when controlling for gestational age among 114 ex-preterm and full-term children.² The present study did not examine visual acuity outcomes, but the more detailed analysis of foveal development from this study may clarify our understanding of visual acuity outcomes in the future.

There are three primary limitations to this study. The first is that infants between 33 and 36 weeks' gestational age were not included due to the practical limitations of imaging that age group. The second limitation is lack of longitudinal follow-up of most infants because imaging only occurred at the time of ROP screenings for preterm infants and once at birth for full-term infants. Additional follow-ups were avoided to prevent further burden on the families and infants. The final limitation is that segmentation using

the MATLAB program for this study was time intensive, limiting usability of this approach in real-life settings. Further algorithm automation is warranted. One strength of this study is that images containing subretinal fluid or cystoid macular edema that altered the foveal contour were excluded, allowing for a cleaner assessment of foveal development. In addition, the semi-automated approach offers a quantitative and more objective analysis of SS-OCT images than subjective assessments. Finally, this study separated the inner and outer retinal layers in analyzing the F/P ratio, identifying that the inner retinal F/P ratio is a more important driver of foveal maturity.

In conclusion, foveal development is a dynamic process that can be partially observed through novel semi-automated analysis of handheld SS-OCT retinal and choroidal imaging in awake infants. Our results demonstrate that foveal angle, inner retinal F/P ratio, and choroidal thickness at the fovea and parafovea are important measures of foveal development.

Acknowledgments

Funded by the Alcon Research Institute Young Investigator Award, Violet Sees, Seattle Children's Research Institute Summer Scholars Program, and unrestricted grants from Research to Prevent Blindness and National Institutes of Health (EY00130) to the University of Washington Department of Ophthalmology.

Disclosure: **S.E. Lawson**, None; **E.K. Tam**, None; **Y. Zheng**, None; **T. Liu**, None; **T.R. Monger**, None; **K.E. Lee**, None; **A. Legocki**, None; **J. Kelly**, None; **L. Ding**, None; **R.K. Wang**, None; **K. Tarczy-Hornoch**, None; **M.T. Cabrera**, None

References

1. Hendrickson A, Possin D, Vajzovic L, Toth CA. Histologic development of the human fovea from midgestation to maturity. *Am J Ophthalmol*. 2012;154(5):767–778.e2.
2. Wu WC, Lin RI, Shih CP, et al. Visual acuity, optical components, and macular abnormalities in patients with a history of retinopathy of prematurity. *Ophthalmology*. 2012;119(9):1907–1916.
3. Akerblom H, Larsson E, Eriksson U, Holmström G. Central macular thickness is correlated with gestational age at birth in prematurely born children. *Br J Ophthalmol*. 2011;95(6):799–803.

4. Wang J, Spencer R, Leffler JN, Birch EE. Critical period for foveal fine structure in children with regressed retinopathy of prematurity. *Retina*. 2012;32(2):330–339.
5. He Y, Pettenkofer M, Chu A, Sadda SR, Corradetti G, Tsui I. Characterization of foveal development in treatment-naïve extremely preterm infants. *Transl Vis Sci Technol*. 2022;11(6):11.
6. Rosén R, Sjöstrand J, Nilsson M, Hellgren K. A methodological approach for evaluation of foveal immaturity after extremely preterm birth. *Ophthalmic Physiol Opt*. 2015;35(4):433–441.
7. O’Sullivan ML, Ying GS, Mangalesh S, et al. Foveal differentiation and inner retinal displacement are arrested in extremely premature infants. *Invest Ophthalmol Vis Sci*. 2021;62(2):25.
8. Song S, Zhou K, Xu JJ, Zhang Q, Lyu S, Wang R. Development of a clinical prototype of a miniature hand-held optical coherence tomography probe for prematurity and pediatric ophthalmic imaging. *Biomed Opt Express*. 2019;10(5):2383–2398.
9. Moshiri Y, Legocki AT, Zhou K, et al. Handheld swept-source optical coherence tomography with angiography in awake premature neonates. *Quant Imaging Med Surg*. 2019;9(9):1495–1502.
10. Huang LC, Zhou H, Legocki AT, et al. Choroidal thickness by handheld swept-source optical coherence tomography in term newborns. *Transl Vis Sci Technol*. 2021;10(2):27.
11. Scoville NM, Legocki AT, Touch P, et al. Vitreous opacities in infants born full-term and preterm by handheld swept-source optical coherence tomography. *J aapos*. 2022;26(1):20.e1–20.e7.
12. Chu Z, Lin J, Gao C, et al. Quantitative assessment of the retinal microvasculature using optical coherence tomography angiography. *J Biomed Opt*. 2016;21(6):66008.
13. de Sisternes L, Hu J, Rubin DL, Marmor MF. Localization of damage in progressive hydroxychloroquine retinopathy on and off the drug: Inner versus outer retina, parafovea versus peripheral fovea. *Invest Ophthalmol Vis Sci*. 2015;56(5):3415–3426.
14. Moreno TA, O’Connell RV, Chiu SJ, et al. Choroid development and feasibility of choroidal imaging in the preterm and term infants utilizing SD-OCT. *Invest Ophthalmol Vis Sci*. 2013;54(6):4140–4147.
15. Li XQ, Munkholm A, Larsen M, Munch IC. Choroidal thickness in relation to birth parameters in 11- to 12-year-old children: The Copenhagen Child Cohort 2000 Eye Study. *Invest Ophthalmol Vis Sci*. 2014;56(1):617–624.
16. Liljequist D, Elfving B, Skavberg Roaldsen K. Intraclass correlation - A discussion and demonstration of basic features. *PLoS One*. 2019;14(7):e0219854.
17. Maldonado RS, Izatt JA, Sarin N, et al. Optimizing hand-held spectral domain optical coherence tomography imaging for neonates, infants, and children. *Invest Ophthalmol Vis Sci*. 2010;51(5):2678–2685.
18. Maldonado RS, O’Connell RV, Sarin N, et al. Dynamics of human foveal development after premature birth. *Ophthalmology*. 2011;118(12):2315–2325.
19. Yanni SE, Wang J, Chan M, et al. Foveal avascular zone and foveal pit formation after preterm birth. *Br J Ophthalmol*. 2012;96(7):961–966.
20. Fieß A, Janz J, Schuster AK, et al. Macular morphology in former preterm and full-term infants aged 4 to 10 years. *Graefes Arch Clin Exp Ophthalmol*. 2017;255(7):1433–1442.
21. Erol MK, Ozdemir O, Turgut Coban D, et al. Macular findings obtained by spectral domain optical coherence tomography in retinopathy of prematurity. *J Ophthalmol*. 2014;2014:468653.
22. Balasubramanian S, Beckmann J, Mehta H, et al. Relationship between retinal thickness profiles and visual outcomes in young adults born extremely preterm: The EPICure@19 Study. *Ophthalmology*. 2019;126(1):107–112.
23. Lee YS, Teh WM, Tseng HJ, Hwang YS, Lai CC, Wu WC. Comparison of foveal thickness in preschool children with a history of retinopathy of prematurity and laser photocoagulation or anti-vascular endothelial growth factor treatment: A prospective, longitudinal study. *Br J Ophthalmol*. 2022;106(1):106–112.
24. Marmor MF, Choi SS, Zawadzki RJ, Werner JS. Visual insignificance of the foveal pit: Reassessment of foveal hypoplasia as fovea plana. *Arch Ophthalmol*. 2008;126(7):907–913.